

# Shear-Based Model for Electron Transport in Hybrid Hall Thruster Simulations

Michelle K. Scharfe, Cliff A. Thomas, David B. Scharfe, Nicolas Gascon, Mark A. Cappelli, and Eduardo Fernandez

**Abstract**—An electron cross-field transport model based on instantaneous simulated plasma properties is incorporated into a radial-axial hybrid simulation of a Hall plasma thruster. The model is used to capture the reduction of fluctuation-based anomalous transport that is seen experimentally in the region of high axial shear in the electron fluid. Similar transport barriers are observed by the magnetic confinement fusion community due to shear suppression of plasma turbulence through an increase in the decorrelation rate of plasma eddies. The model assumes that the effective Hall parameter can be computed as the sum of the classical term, a near-wall conductivity term, and a fluctuation-based term that includes the effect of shear. A comparison is made between shear-based, experimental, and Bohm-type models for cross-field transport. Although the shear-based model predicts a wider transport barrier than experimentally observed, overall, it better predicts measured plasma properties than the Bohm model, particularly in the case of electron temperature and electric potential. The shear-based transport model also better predicts the breathing-mode oscillations and time-averaged discharge current than both the Bohm and experimental mobility models. The plasma property that is most sensitive to adjustment of the fitting parameters used in the shear-based model is the plasma density. Applications of these fitting parameters in other operating conditions and thruster geometries are examined in order to determine the robustness and portability of the model. Without changing the fitting parameters, the simulation was able to reproduce macroscopic properties, such as thrust and efficiency, of an SPT-100-type thruster within 30% and match qualitative expectations for a bismuth-fueled Hall thruster.

**Index Terms**—Anomalous transport, electron shear, Hall-effect devices, propulsion, simulations.

Manuscript received November 9, 2007; revised February 25, 2008. First published October 31, 2008; current version published November 14, 2008. This work was supported in part by the U.S. Air Force Office of Scientific Research. The work of M. K. Scharfe was supported by the Stanford Graduate Fellowship Program, and that of D. B. Scharfe was supported by the National Science Foundation Graduate Research Fellowship Program.

M. K. Scharfe, D. B. Scharfe, and M. A. Cappelli are with the Mechanical Engineering Department, Stanford University, Stanford, CA 94305 USA (e-mail: mkallis@stanford.edu).

C. A. Thomas was with the Mechanical Engineering Department, Stanford University, Stanford, CA 94305 USA. He is now with Lawrence Livermore National Laboratory, Livermore, CA 94550 USA.

N. Gascon was with the Mechanical Engineering Department, Stanford University, Stanford, CA 94305 USA. He is now with Space Systems/Loral, Palo Alto, CA 94303 USA.

E. Fernandez is with the Department of Mathematics and Physics, Eckerd College, St. Petersburg, FL 33711 USA.

Color versions of one or more of the figures in this paper are available online at <http://ieeexplore.ieee.org>.

Digital Object Identifier 10.1109/TPS.2008.2004364

## I. INTRODUCTION

THE EFFICIENT operation of plasma propulsion devices relies on their ability to ionize neutral gas and accelerate the ions to high exhaust velocities using electric and magnetic fields. In a coaxial Hall effect thruster, ions are accelerated using an externally applied electric field, while electrons are axially trapped in an azimuthal  $E \times B$  Hall current caused by an imposed radial magnetic field. The mechanism by which electrons traverse magnetic field lines is an area of considerable research. Experimentally, the electron conductivity in these devices is observed to be higher than predicted based on electron collisions with heavy particles [1]. Possible explanations for the anomalous conductivity are near-wall transport [2], [3] and azimuthal fluctuations [4], both of which increase the effective collision frequency of electrons.

An accurate model for electron transport is critical for the development of a Hall thruster simulation with predictive capabilities. One common method for describing anomalous cross-field transport involves using a fluctuation-based Bohm-type model that scales inversely with the magnetic field (unlike the  $1/B^2$  dependence of the classical collision model). While this method is in reasonable agreement with experiment for most regions of the thruster channel, there exists a region near the peak in magnetic field where the electron mobility is experimentally observed to be nearly classical [1]. This region of lower electron conductivity, which occurs in a region of strong gradients, is somewhat paradoxical in that instabilities causing fluctuation-induced transport are typically enhanced by gradients in properties such as plasma density [5]. One possible explanation for this transport barrier is that it is caused by the axial gradient in azimuthal electron velocity, which is maximized in the same region [6].

Support for this idea is provided by many fusion applications, such as tokamaks and stellarators, which exhibit similar confinement phenomena in regions of strong shear. It is believed that the anomalous conductivity caused by fluctuations is suppressed in regions where the flow is sheared due to the stretching and consequent decorrelation of turbulent eddies [7]. It should be noted that Hall thruster plasmas are, in fact, very different from magnetic fusion devices such as these. For example, the sheared flow in Hall thrusters is an electron flow, while in tokamaks, ions are magnetized as well. Also, unlike fusion applications, Hall thrusters exhibit a complex shear structure which includes a zero crossing. Additionally, some fluctuations in a Hall thruster are likely advected out of the shear region faster than the eddy turnover time. However, motivation for application of shear transport suppression is provided by the

apparent universality and robustness of this mechanism in numerous devices with differing magnetic field configurations.

An accurate description of the relation between flow shear and the transport barrier will allow not only more accurate simulations but also a means to further optimize thruster performance. A steeper transport barrier will result in a narrower and stronger axial electric field, possibly decreasing plume divergence and ion-induced channel erosion [8]. Also, favorable placement of the barrier downstream of the ionization zone may increase propellant utilization efficiency. In order to numerically capture the transport barrier due to shear, an empirical model based on observations by the magnetic fusion community [9], [10] and a simplified linear analysis [11] has been implemented in a radial–axial hybrid simulation of a Hall thruster.

The hybrid model treats the heavy species kinetically while neglecting electron kinetic effects by treating the electrons as a fluid. Section II provides descriptions of the numerical hybrid simulation and the shear transport model, while Section III presents the results of the shear model through a comparison with other transport models and a sensitivity analysis of the fitting parameters and simulation assumptions. An examination of the utility and portability of this model with a given set of fitting parameters to simulations of an SPT-100 and bismuth Hall thruster is also provided in Section III.

## II. NUMERICAL MODEL

### A. Hybrid Simulation

The hybrid particle-in-cell (PIC) simulation into which the shear-based model for cross-field electron transport is incorporated is a 2-D (radial–axial) model of the interior channel and near-field region of a laboratory Hall thruster, referred to here as the Stanford Hall thruster [12]. A brief description of the numerical model is given hereafter. A more detailed description is provided in [13].

The simulated geometry corresponds to a thruster with an annular channel of 8 cm in length, 1.2 cm in width, and with an outer diameter of approximately 9 cm. In the hybrid model, the electrons are treated as a quasi-1-D fluid, while the heavy species are treated as discrete particles advanced in space using a PIC approach. The two solutions are coupled assuming space-charge neutrality.

The electron fluid is governed by the first three moments of the Boltzmann equation, as described by Fife [14]. The electron continuity equation is enforced through current continuity, where the instantaneous discharge current is determined in order to satisfy the potential boundary conditions at the anode and cathode. The electron momentum equation is solved in the two directions parallel and perpendicular to the magnetic field. Along magnetic field lines, infinite conductivity is assumed resulting in a balance between electric and pressure forces. In the perpendicular direction, an effective Hall parameter is used to determine the electron velocity in order to account for the anomalously high electron cross-field conductivity relative to classical diffusion. The following three separate models for the Hall parameter have been implemented in the simulation and will be examined in Section III-A: an empirical shear-

based calculation, an experimentally measured profile [1], and a Bohm-type model [15].

Imposing a uniform temperature along magnetic field lines, a 1-D energy equation is solved to calculate the electron temperature. The unsteady spatially varying electron energy equation includes thermal conduction and flow work, as well as source and sink terms due to joule heating, ionization, and heat loss to the channel walls. Although the sheath is not directly simulated in the quasineutral model, a simplified analysis based on the simulated ion flux to the wall is used to calculate the sheath potential in order to determine energy losses. The non-Maxwellian nature of the electron species is included in an *ad hoc* manner using an effective electron temperature which is lower than the simulated temperature perpendicular to the magnetic contours, as described in [13]. In addition to the electron cross-field velocity description, heat conduction is also modeled using the anomalous conductivity. The electron temperature is coupled to the electric field through current continuity.

The axisymmetric heavy-particle species are advanced in time through solution of their respective equations of motion in cylindrical coordinates. Due to the large Larmor radius of the ion species, the force produced by the magnetic field on the ions is neglected. Neutral injection occurs from the center of the anode, as well as from the boundaries of the plume to simulate background gas, with a distribution based on a one-way Maxwellian flux. Electron impact ionization of neutral particles is modeled using local densities and the electron temperature. Heavy particles which impact channel walls are assumed to reflect diffusely at the wall temperature, while ions are additionally assumed to recombine into neutrals upon impact. Charge-exchange collisions occur throughout the domain.

The simulation is initialized with approximately 500 000 neutral superparticles and 200 000 ion superparticles, where each superparticle represents between  $10^8$  and  $10^{12}$  actual particles. The temperature profile and current are also initialized and used to calculate an initial electric field. The heavy particles are updated individually through a second-order solution of the equation of motion for each superparticle. Neutral particles are injected from the anode and plume based on the prescribed mass flow rate of 2 mg/s and background pressure of 0.05 mtorr, while charge-exchange collisions are simulated using a direct-simulation Monte Carlo approach. The electron temperature is updated using a fourth-order Runge–Kutta scheme satisfying the imposed boundary conditions of no heat transfer at the anode and prescribed temperature at the cathode. The computed temperature profile is used to update the potential, and the discharge current is modified as necessary to satisfy the potential boundary conditions. Due to the fast electron time scale relative to the ions and neutrals, the time step used for the electrons is 0.1 ns, while the heavy particles are advanced after several electron iterations with a time step of 25 ns. On a 3.8-GHz Pentium 4 processor, the simulation completes 625  $\mu$ s, or approximately five to ten “breathing-mode” cycles [16], in two days.

### B. Shear-Based Transport Model

Experimental measurements of the electron cross-field mobility, an example of which is shown in Fig. 1, illustrate that the

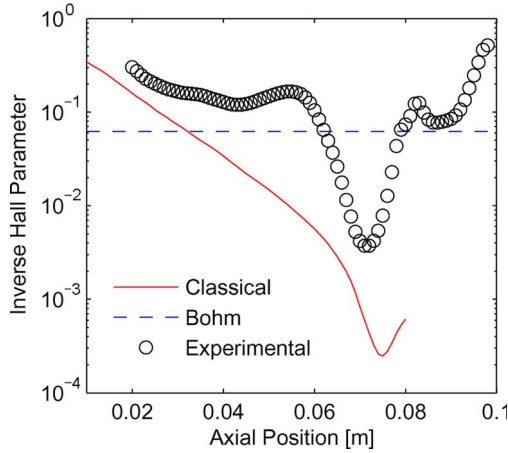


Fig. 1. Experimental inverse Hall parameter is compared with the classical value based on experimental collision rates and the Bohm values at a discharge voltage of 200 V.

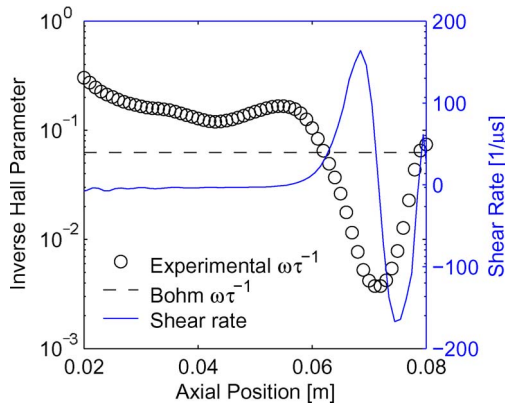


Fig. 2. Experimental measurements of inverse Hall parameter and axial electron shear rate at 200-V discharge voltage.

effective Hall parameter  $\omega\tau_{\text{eff}}$  (i.e., determined by experiments) is considerably higher than the classical value in most regions of the Hall thruster channel [1]. It should be noted that there exists a large amount of experimental uncertainty leading to possible error in the experimental value of up to an order of magnitude. Even accounting for this uncertainty, it is clear that a region exists near the exit plane of the thruster, located at 0.08 m, where the transport approaches the classical value. As shown in Fig. 2, this region of decreased transport overlaps with a region of strong electron axial shear [6]. Similar transport barriers in the region of high shear have also been observed experimentally in magnetic confinement fusion devices over the last two decades [17], [18].

Due to the importance of the transport barrier in magnetic fusion applications for reasons such as plasma confinement and reduction of radial heat flux across closed magnetic surfaces, the phenomenon of reduced transport due to shear has been extensively studied. It has been analytically shown that electron diffusion is decreased due to a reduction in the turbulent fluctuation amplitudes as well as a modification of the phase difference, or cross phase, between fluctuations in plasma properties which cause transport, such as plasma density and electron velocity [19]–[22].

Qualitatively, the shear turbulence suppression mechanism is a result of the stretching and distortion of turbulent eddies which are caused by the position-dependent velocity of fluid elements within the eddy. The distortion results in an effective decrease in the eddy lifetime, lowering the time scale from the eddy turnover time to the inverse shear rate, and a decrease in the correlation length in the direction of transport [7]. Also, it has been suggested that the shearing of the flow improves the overall stabilization of the system by coupling unstable modes to nearby stable modes leading to a reduction in transport [23]. The universal nature of the turbulence suppression mechanism extends to nonionized fluids as well as plasmas. Although not common in hydrodynamics, a similar phenomenon is observed in large-scale turbulence in the stratosphere [24].

Due to the complicated nature of the nonlinear process, a number of different transport models have been suggested to describe this reduction of transport. The model examined in this paper, and in our previous work [25], is of the form [9], [10]

$$(\omega\tau)_{\text{eff}}^{-1} = (\omega\tau)_{\text{clas}}^{-1} + (\omega\tau)_{\text{nw}}^{-1} + (\omega\tau)_{\text{fluc}}^{-1} \left( \frac{1}{1 + (Cs)^\alpha} \right) \quad (1)$$

where  $\omega\tau_{\text{clas}}$  is the classical Hall parameter based on electron neutral collisions,  $\omega\tau_{\text{nw}}$  is the near-wall term based on the electron collision rate with channel walls,  $\omega\tau_{\text{fluc}}$  describes the transport due to fluctuations, and the shear rate  $s$  is given by

$$s = \frac{du_{e,\theta}}{dz} = \frac{dE_z/B_r}{dz} \quad (2)$$

In (2), the azimuthal electron velocity due to radial electric and axial magnetic fields has been neglected. Note that this equation would not be applicable if the electrons were unmagnetized. When the empirical exponent in the shear term,  $\alpha$ , is set equal to two, this form is consistent with a linearized calculation performed by Thomas [11]. Although the original Bohm value [15] of  $\omega\tau_{\text{fluc}}$  is 16, the transport using this value was found to be too low in the radial–axial hybrid simulation. Therefore, this term was treated as an adjustable fitting parameter. The coefficient  $C$  represents the turbulence decorrelation time in the absence of shear, which is related to the growth rate of the instability causing transport. As this value is not known and may depend on a number of nonlinear effects,  $C$  is also treated as a fitting parameter.

As previously mentioned, due to the nonlinear nature of the plasma behavior, other empirical forms for the reduction in transport have been suggested by the fusion community [26], [27]. The effect of one such model has been examined in a radial–axial fully kinetic Hall thruster simulation by Fox *et al.* [28]. To begin to understand the sensitivity of the form chosen in (1), the exponential dependence of the shear term,  $\alpha$ , was varied from the default value of two, and results are presented in Section III-B.

Using the chosen fitting parameters, at each time step, the effective Hall parameter  $\omega\tau_{\text{eff}}$  is calculated using simulated plasma properties to compute  $\omega\tau_{\text{clas}}$ ,  $\omega\tau_{\text{nw}}$ , and  $s$ . Since the shear is based on the second derivative of the computed potential, a spline fit is used to compute this derivative to avoid anomalously high shear values caused by numerical noise.

Also, the Hall parameter is only calculated along the center of the channel and assumed to be radially uniform.

At present, three simplifying assumptions are made to both reduce computational cost and increase numerical stability. First, the Hall parameter outside the channel is assumed constant at the value specified by the fitting parameter  $\omega\tau_{\text{fluc}}$ . This assumption is partially supported by the findings of Smith and Cappelli [29], which suggest that, outside the thruster, nonlocal electron motion due to strong spatial variations in both the electric and magnetic field drives transport to levels comparable to Bohm values. Second, the updating of the effective Hall parameter is under-relaxed, resulting in an instantaneous Hall parameter that contains remnant effects from the previous time steps. Last, the instantaneously computed Hall parameter is smoothed spatially in the axial direction for increased numerical stability. It is believed that, physically, sharp gradients in the axial direction would be smoothed by variations in the azimuthal dimension that are not captured by the radial-axial simulation. The effect of these assumptions on the results is discussed in the following section.

### III. RESULTS AND DISCUSSION

#### A. Comparison of Transport Models

Using simulated plasma properties computed with the experimentally measured mobility, initial values of the fitting parameters  $C$  and  $\omega\tau_{\text{fluc}}$  were chosen such that the initial computed mobility using the shear-based transport model was in good agreement with experimental measurements. The exponential dependence, defined by fitting parameter  $\alpha$ , was assumed to be quadratic. However, when a shear-based conductivity model was implemented using these fitted coefficients, the plasma properties used to optimize the parameters were modified due to the change in electron transport. The coefficients were therefore adjusted to produce better qualitative agreement between simulated and measured plasma properties.

At a discharge potential of 200 V, fitting parameters which were observed to provide reasonable agreements with experimental measurements were  $\omega\tau_{\text{fluc}} = 8$  and  $C = 16 \times 10^{-8}$  s. Using these parameters, the computed inverse Hall parameter was found to have a “well” about half as deep and twice as wide as experimentally observed, as shown in Fig. 3. Note that the implemented inverse Hall parameter outside the channel is fixed to a constant Bohm-like value. While the near-wall conductivity is found to have an influence in the region near the exit plane of the thruster, located at 0.08 cm, the shape of the computed average inverse Hall parameter is primarily determined by the contribution from the term based on shear suppression of fluctuation-induced transport.

As shown by Fig. 4(a), the shear-based model for electron transport accurately captures the location of the peak in electron temperature, unlike the Bohm model. While the experimental mobility slightly overpredicts the peak value of electron temperature, the shear-based model slightly underpredicts this value to a lesser degree. Note that the experimental uncertainty in the measured electron temperature is approximately  $\pm 1$  eV.

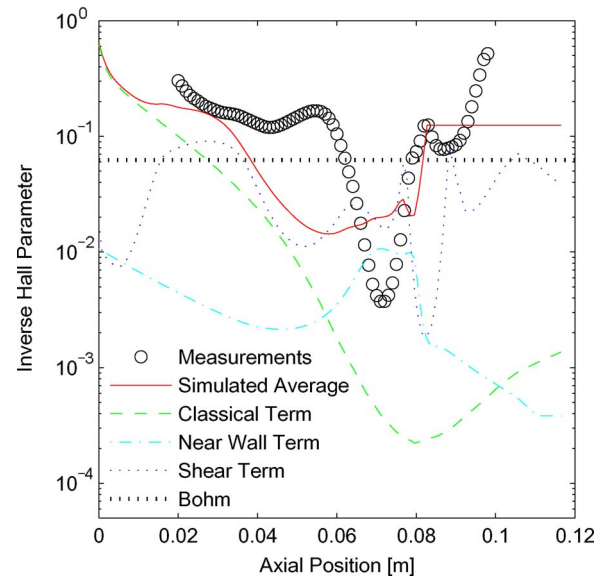


Fig. 3. Experimentally measured inverse Hall parameter is compared with the Bohm value and the average computed value. The simulated average is based on classical, near-wall, and shear-based contributions.

Fig. 4(b) shows the effect of Bohm, experimental, and shear-based transport models on the electric potential. The experimental uncertainty in the measured potential at each location is approximately  $\pm 5$  V. The steep temperature profile produced by the experimental mobility, as shown in Fig. 4(a), produces a potential drop which is steeper than experimental observations, resulting in a high electric field. While the Bohm mobility produces similar electric fields to experiments, the potential drop occurs farther downstream than expected. The shear model, on the other hand, predicts moderate electric fields occurring approximately in the location experimentally observed. It should be noted that while the shear-based transport model predicts the potential reasonably well, the corresponding ion acceleration is found to be broader than experimentally measured.

As shown by Fig. 5, the time-varying shear-based model for electron mobility produces higher frequency fluctuations in the discharge current than experimentally observed or predicted by the experimental and Bohm mobility models. However, the shear-based model also exhibits distinct and large-amplitude breathing-mode cycles similar to experimental measurements. Of the three models for electron transport, at a 200-V discharge voltage, the shear model produces the best agreement with the time-averaged experimental discharge current. This may, however, be coincidental since other properties, such as plasma density, are most accurately computed using the experimental mobility. While the Bohm mobility predicts an average current of 6.1 A and experimental mobility predicts 1.8 A, the computed shear-based model predicts an average of 3.2 A compared to the experimental value of 2.7 A.

#### B. Sensitivity Analysis

To illustrate the shear-based transport model at a variety of discharge voltages, this section presents results at a discharge

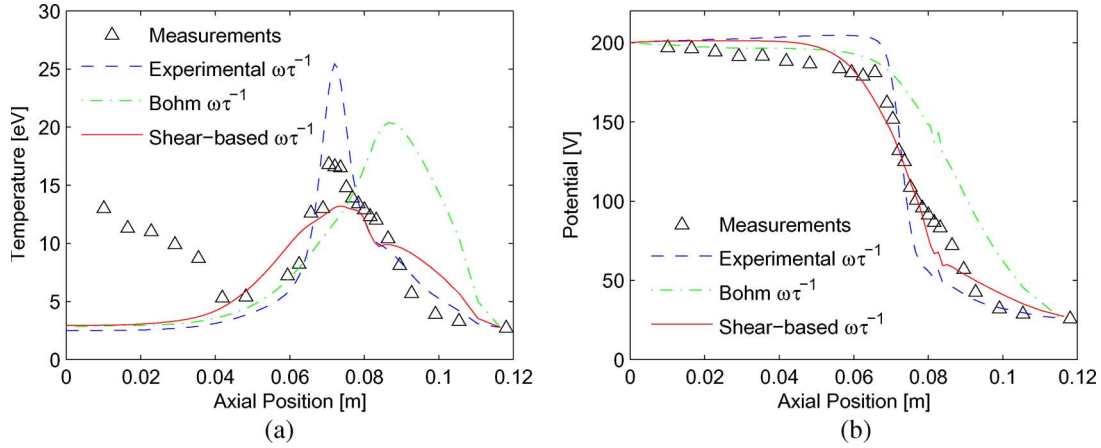


Fig. 4. Comparison between measured and simulated plasma properties using Bohm, experimental, and shear-based models for electron transport. (a) Electron temperature. (b) Potential.

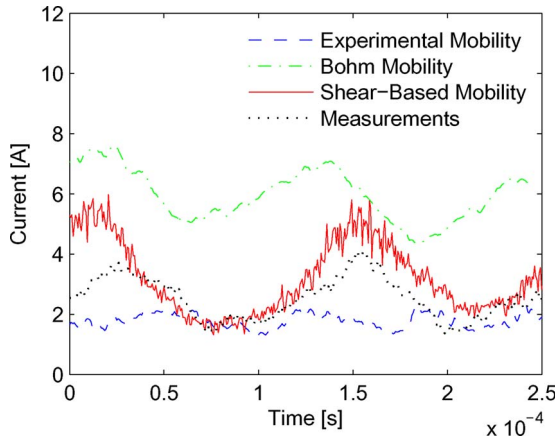


Fig. 5. Comparison of simulated discharge currents using Bohm, experimental, and shear-based models for electron transport.

voltage of 160 V, while the previous section used a discharge voltage of 200 V.

1) *Fitting Parameters:* The two fitting parameters  $C$  and  $\omega\tau_{fluc}$  were chosen somewhat arbitrarily at each discharge voltage to produce reasonable agreement with experimental measurements. While the baseline value  $\omega\tau_{fluc}$  performed equally well at different discharge voltages, lower values of the coefficient  $C$  were found to be more appropriate at lower voltage. This implies that the baseline transport due to fluctuations in the absence of shear is relatively independent of voltage, while the decorrelation time of turbulent eddies in the absence of shear increases with increasing voltage.

The sensitivity to adjustments of the parameters has been found to be relatively small for properties such as potential, electron temperature, and neutral and ion velocities. The plasma property that is most sensitive to alteration of these parameters is the plasma density. The variations in plasma density due to changes in  $\omega\tau_{fluc}$  and  $C$  are shown in Fig. 6. While the chosen value of  $C$  in the empirical model seems to have a considerable effect on plasma density, the effect of the base fluctuation Hall parameter  $\omega\tau_{fluc}$  was found to be fairly small.

As shown in Fig. 6(a), the plasma density increases slightly as  $\omega\tau_{fluc}$  is decreased. This is expected since a lower baseline

Hall parameter corresponds to a higher mobility. The increased conductivity of electrons leads to a higher current density which produces more Joule heating. The increased heating causes higher temperatures and larger ionization rates leading to an increased plasma density. However, as shown by Fig. 6(a), this effect appears to be small. Note that the experimental uncertainty in measured plasma density is approximately  $\pm 10^{17} \text{ m}^{-3}$ .

As shown in Fig. 6(b), the plasma density also increases as  $C$  is decreased. Based on the form of (1), this is expected since the fluctuation-induced transport is further suppressed as the value of  $C$  is increased. However, while changes in  $C$  produce large effects on the plasma density, both in the magnitude and location of the peak value, the effects are less significantly observed in other plasma properties such as electron temperature and potential.

Since the observed “well” in the computed inverse Hall parameter is wider than predicted by experimental measurements, the effect of the exponential dependence of the shear in the assumed form [(1)] has also been examined. The exponential fitting parameter  $\alpha$  was increased from the value of two used in the previous analysis in order to make the dip in the inverse Hall parameter more narrow. While increasing  $\alpha$  had the effect of narrowing the barrier, as shown in Fig. 7, the effect was small for each incremental increase in  $\alpha$ . Using this form for the experimental inverse Hall parameter would require a high-order exponential dependence to produce a transport barrier as narrow as the one experimentally observed.

2) *Simplifying Assumptions:* As mentioned in Section II-B, three assumptions were implemented in the simulation with the primary intent of increasing numerical stability. Namely, the inverse Hall parameter was held constant in the near-field region, under-relaxed, and spatially averaged.

In the results presented in the previous sections, the shear model has only been implemented up to the exit plane, as shown in Fig. 3. Beyond the exit plane, the Hall parameter was assumed to be constant at the baseline value  $\omega\tau_{fluc}$ . Also, in these results, the Hall parameter was not computed using the instantaneous plasma properties but was rather under-relaxed by combining 40% of the instantaneous value with 60% of the value implemented at the previous time step. Lastly, a five-point

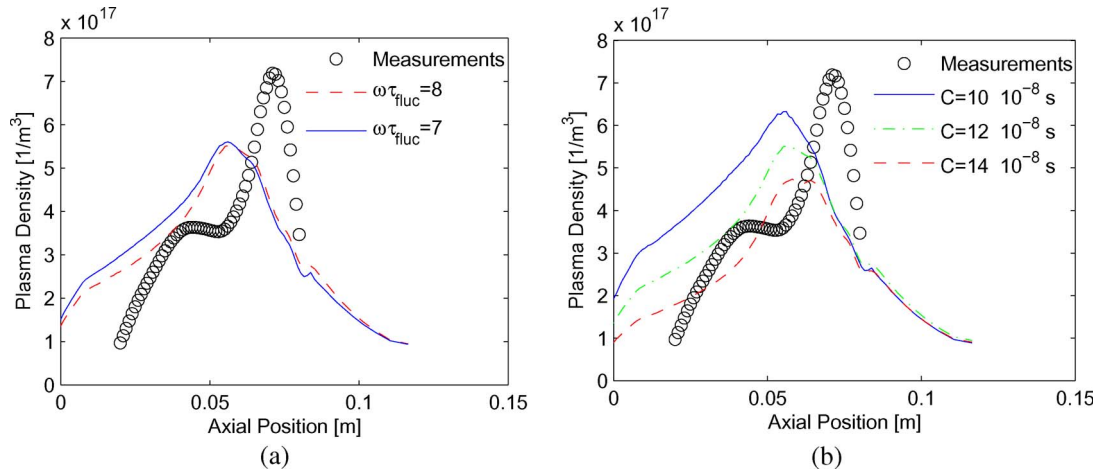


Fig. 6. Trend observed in plasma density due to variation of fitting parameters at a discharge voltage of 160 V. (a)  $\omega\tau_{fluc}$ . (b)  $C$ . In (a),  $C$  is held constant at  $12 \times 10^{-8}$  s, while in (b),  $\omega\tau_{fluc}$  is held constant at eight.

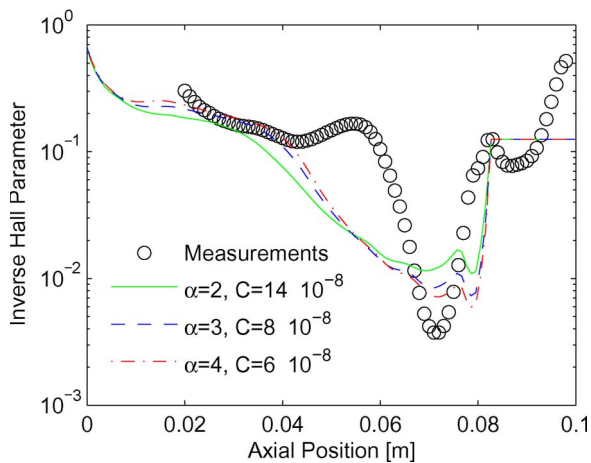


Fig. 7. Trend observed in the time-averaged inverse Hall parameter due to variation of exponential fitting parameter  $\alpha$  at discharge voltage of 160 V.  $\omega\tau_{fluc}$  is held constant at eight, and  $C$  is modified to produce similar average values.

Gaussian-like weighting was used to spatially average the instantaneously computed Hall parameter. The effect of these assumptions is described hereafter.

As shown in Fig. 8(a), the transition location in the near-field region from the shear-based model to a constant inverse Hall parameter has little effect on the values upstream of the exit plane, located at 0.08 m. However, the increased transport barrier outside the thruster results in the potential drop moving slightly farther downstream. The higher electric field in the near-field region results in more Joule heating, causing the temperature to be higher outside the thruster, as shown in Fig. 8(b). However, as most of the ionization is accomplished inside the channel, the effect of this increased temperature outside the thruster is small.

Although the transition location had only a small effect on the time-averaged simulated plasma properties, the effect on the instantaneous properties was much more significant. One issue with the model in its present form is that it is inherently unstable due to the zero-crossing in shear, which can be seen in Fig. 2. A single smooth transport barrier, such as the one shown in Fig. 2,

produces two maxima in shear. These two maxima produce two transport barriers located on either side of the original barrier. This process results in complicated waves which travel axially in both directions and are limited in speed only by the numerical limitations of the time step.

When the transition to a Bohm-like Hall parameter is located at the exit plane, the waves move primarily to the left, as shown in Fig. 9(a). However, when the transition location is moved farther downstream, waves are free to propagate in both directions, as shown in Fig. 9(b). Although it is unknown whether these waves have any physical basis or are simply numerical, they seem to have little influence on the time-averaged behavior. Changing the time step modifies the speed of these disturbances but does not alter the time-averaged plasma properties.

As shown by Fig. 9, the computed Hall parameter is very dynamic. The instantaneous Hall parameter profiles have features which are narrow and deep, resembling the experimentally observed Hall parameter. However, since these features travel over regions on the order of centimeters, the time-averaged computed Hall parameter is broad and shallow. Because the instantaneous Hall parameter does not resemble its time-averaged value, under-relaxing the computed Hall parameter has a significant effect on simulated plasma properties.

For large amounts of time averaging, the computed inverse Hall parameter is considerably lower than the experimental value and peaks too far upstream, as shown in Fig. 10(a). As the proportion of the instantaneous Hall parameter used to update the mobility is decreased, the transport barrier is reduced, and the mobility becomes more Bohm-like. This results in plasma properties which more greatly resemble those simulated using a Bohm mobility, such as a greater potential drop outside the thruster, a decreased backflow region, an increased plasma density near the anode, and an increased electron temperature in the near-field region, as shown in Fig. 10(b). Decreasing time averaging beyond a 40% weighting of the instantaneous value results in increased numerical instability.

Spatial averaging, however, has little effect on the simulated results. While most plasma properties remain essentially unchanged by the different center-dominated weighting schemes,

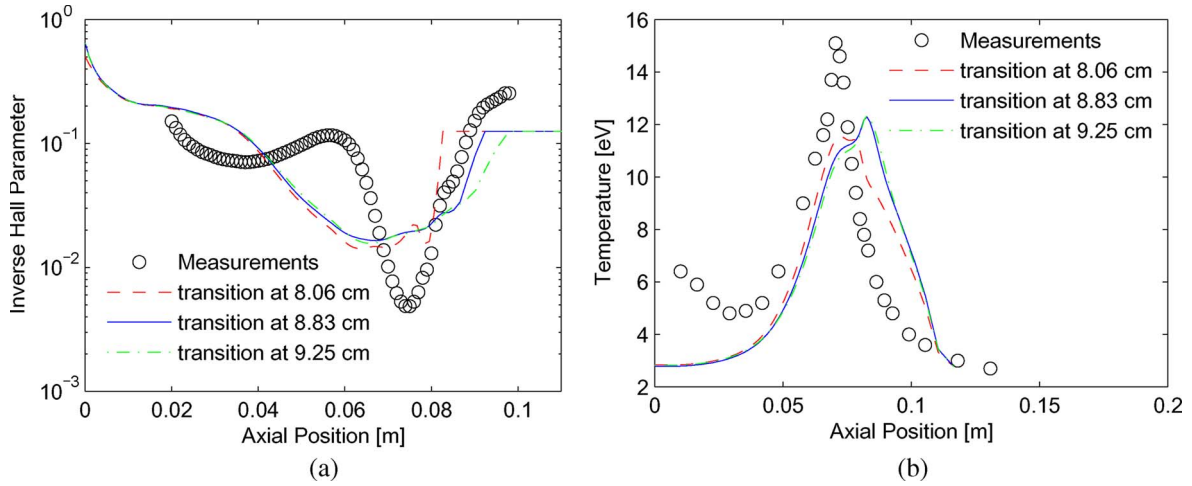


Fig. 8. Effect of the location defining the transition from the shear-based model for electron transport to a constant inverse Hall parameter in the near-field region at a discharge voltage of 160 V. (a) Time-averaged inverse Hall parameter. (b) Electron temperature. Note that  $C = 12 \times 10^{-8}$  s, while  $\omega\tau_{fluc} = 8$ .

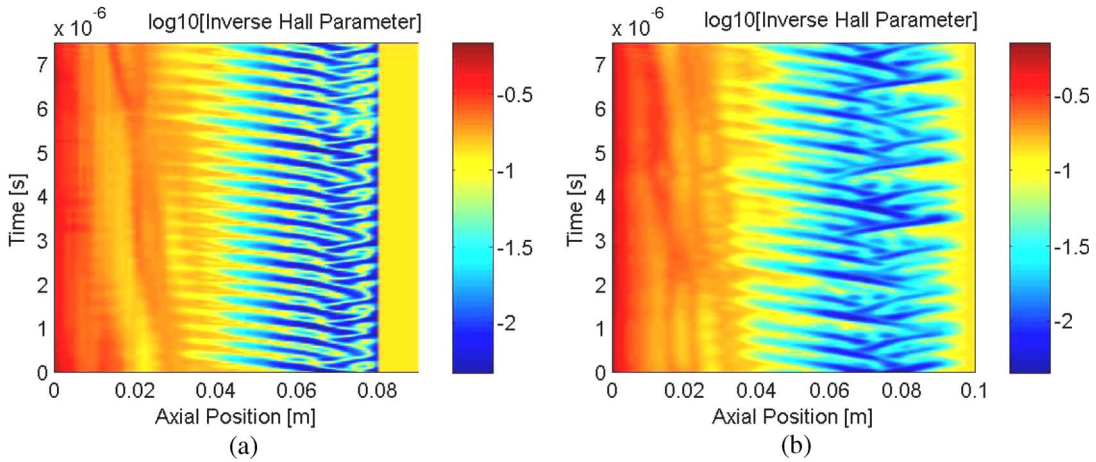


Fig. 9. Waves observed in the computed inverse Hall parameter at a discharge voltage of 160 V. (a) Transition to constant Hall parameter located at 8.06 cm. (b) Transition to constant Hall parameter located at 8.83 cm. Note that  $C = 12 \times 10^{-8}$  s, while  $\omega\tau_{fluc} = 8$ .

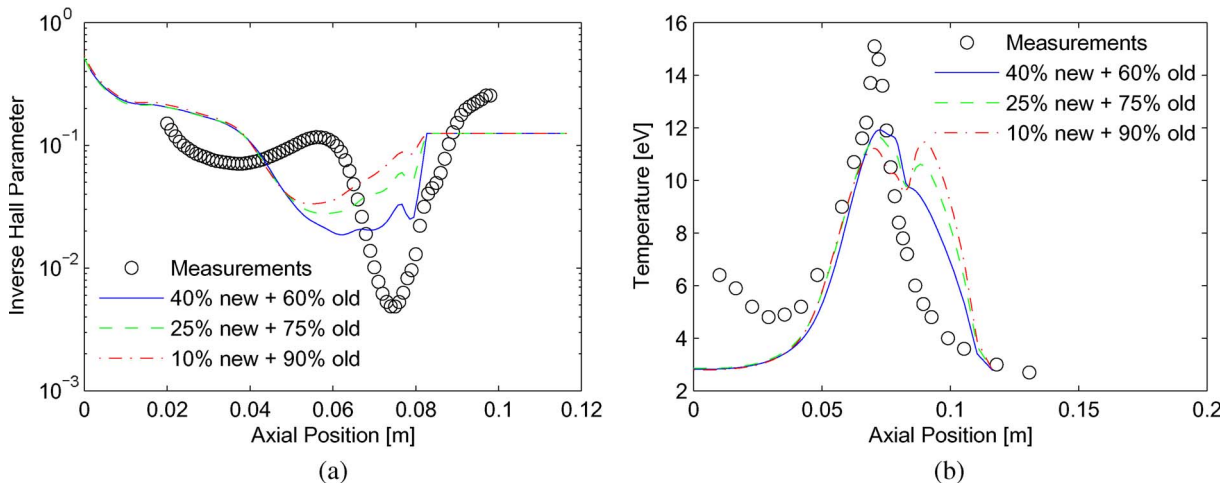


Fig. 10. Effect of time averaging of computed mobility at a discharge voltage of 160 V. (a) Inverse Hall Parameter. (b) Electron temperature. Note that  $C = 12 \times 10^{-8}$  s, while  $\omega\tau_{fluc} = 8$ .

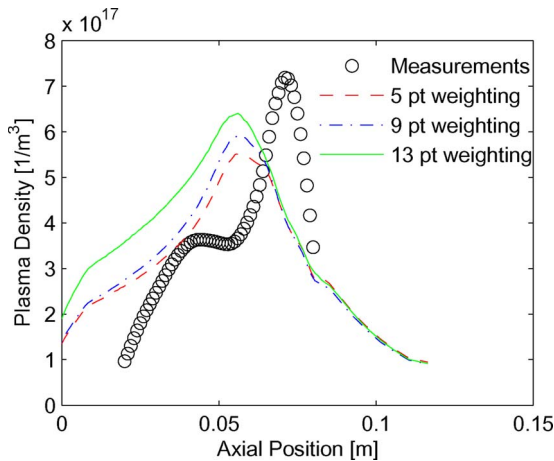


Fig. 11. Effect of spatial weighting on simulated plasma density.

the plasma density is the property that is most greatly affected. As shown in Fig. 11, an increase in the number of points used in a center-dominated weighting scheme from 5 to 13, which represents an increase in scale from approximately 5 mm to 1.3 cm, causes an increase in peak plasma density of approximately 20%.

### C. Applications of Shear-Based Transport Model

While, physically, it is expected that the values of  $C$  and  $\omega\tau_{\text{fluc}}$  will vary for different operating conditions and thruster geometries, an attempt has been made to examine the transportability of these parameters to simulations other than the one for which they were optimized. Although the parameters are likely dependent on plasma properties and characteristics of the instability causing transport, they provide a starting point for describing the transport barrier in thrusters for which an experimental mobility has not been measured.

1) *SPT-100*: In order to assess the validity and utility of the transport model, the shear-based model for inverse Hall parameter was implemented in simulations of an SPT-100 geometry thruster using the fitting parameters  $C = 16 \times 10^{-8}$  s,  $\omega\tau_{\text{fluc}} = 8$ , and  $\alpha = 2$ . Simulations were run consistently with the operating conditions described in the evaluation of the Russian SPT-100 thruster at NASA [30], and results are compared in Table I with experimental measurements of discharge current, thrust, and total efficiency. Although the discharge voltage, anode flow rate, and facility background pressure could be reproduced in the simulation, the cathode flow rate, which was varied in the experimental measurements, is not captured by the hybrid simulation. Therefore, in the results presented, the experimental total efficiency has been recalculated using the results for a cathode flow rate of 0.25 mg/s. Total efficiency  $\eta$  is given by

$$\eta = \frac{T^2}{2\dot{m}IV} \quad (3)$$

where  $T$  is the thrust,  $\dot{m}$  is the flow rate (taken to be the anode flow rate),  $I$  is the discharge current, and  $V$  is the discharge voltage.

As shown by Table I, at a discharge voltage of 200 V, the efficiency is calculated with remarkable accuracy. However, the simulation overestimates the thrust by approximately 30% for both anode flow rates. The ability of the simulation to maintain the correct efficiency while overpredicting the thrust is attributed to a simulated discharge current which is a factor of 1.8 too high for both mass flow rates. The elevated current implies a higher plasma density, which produces higher thrust.

At a discharge voltage of 250 V and an anode flow rate of 4.64 mg/s, the thrust is overestimated by 13%, while the efficiency is underestimated by 25%. The lower simulated efficiency despite the higher simulated thrust relative to experimental measurements is attributed to a simulated discharge current which is slightly more than two times too high. This implies that the value of  $C$  implemented at 250 V is substantially too low. Small values of  $C$  typically produce more Bohm-like behavior, with the maximum in electron temperature increasing in magnitude and moving outside the channel. The overprediction of peak temperature results in a large plasma density and, therefore, a large discharge current and increased thrust. However, because the peak temperature occurs too far downstream, ionized particles do not accelerate through the full potential drop, decreasing thrust and lowering efficiency.

The value of  $C$  implemented in the SPT-100 was chosen as the value which produced reasonable agreement with experimental measurements of the Stanford Hall thruster. However, as the two types of thrusters utilize different magnetic field configurations, geometries, and operating conditions, it is unlikely that the value of  $C$  would be directly transferable. The instabilities which produce transport and the decorrelation rate in the absence of shear are likely a function of specific thruster geometry and operating conditions. Although the value of  $C$  implemented in the transport model was likely appropriate for a discharge voltage of 200 V in the Stanford Hall thruster, better agreement for the SPT-100, particularly in the area of discharge voltage, can be obtained by increasing the value of  $C$  at the same discharge voltage.

Also, for consistency, the value of the fitting parameter  $C$  was kept the same in the simulation of an SPT-100 at both discharge voltages. However, as was noted in Section III-B-1, higher values of  $C$  are found to be more appropriate at higher voltages. A larger value of  $C$  will result in a deeper transport barrier, which will have the effect of lowering the simulated discharge current. Therefore, it should be noted that the  $C$  value implemented in Table I, which is based on the Stanford-Hall-thruster 200-V operating conditions, is expected to be more inaccurate at 250 V than at 200 V.

Despite the lack of quantitative agreement, the observed trends with varying discharge voltages and mass flow rates are qualitatively aligned between simulations and measurements. Thrust increases with both increasing anode flow rate and increasing discharge voltage. Although, experimentally, the thrust increases by a much larger amount than simulated, at the higher cathode flow rate of 0.5 mg/s, the increase in thrust is less than 10% when the discharge voltage is increased from 200 to 250 V, in better agreement with simulated results. Efficiency is found to be relatively independent of anode flow rate. At a 200-V discharge voltage and a higher cathode flow rate of 0.5 mg/s,

TABLE I  
COMPARISON OF SIMULATED AND EXPERIMENTALLY MEASURED PERFORMANCE PARAMETERS OF AN SPT-100 HALL THRUSTER

Discharge Voltage [V]	Anode Flow Rate [mg/s]	Current [A]		Thrust [N]		Efficiency	
		Sim.	Exp.	Sim.	Exp.	Sim.	Exp.
200	5.05	7.8	4.5	0.074	0.058	0.38	0.37
200	3.61	5.3	3.0	0.051	0.040	0.36	0.37
250	4.64	8.4	4.0	0.078	0.069	0.33	0.44

the total efficiency is experimentally found to decrease by 3% as the anode flow rate is lowered from 5.05 to 3.56 mg/s, similar to the observed decrease of 5% in the simulated results shown in Table I. While the efficiency did not increase as expected at 250 V, this is attributed to an implemented  $C$  value which is more greatly underestimated at 250 V than at 200 V.

2) *Bismuth Thruster*: An additional test of the portability of the proposed transport model was performed by implementing the model in simulations of a bismuth-fueled Hall thruster. The use of bismuth as a Hall thruster propellant was studied in the former U.S.S.R. four decades ago, and there has been recent renewed interest in developing such technology in the U.S. [31]. The Russian-developed bismuth thrusters have numerous advantages over modern xenon thrusters [31]–[33], including higher thrust and more advanced two-stage designs. The bismuth propellant itself lends significant advantages to Hall thruster performance. For example, bismuth 209 is the heaviest of all radioactively stable isotopes and is nearly 60% more massive than xenon, providing an additional 26% of thrust per accelerated ion at a given thruster voltage. The ionization energy of bismuth is 40% lower than that of xenon, providing more efficient ionization. Furthermore, bismuth is condensible at room temperature, providing reduced spacecraft tankage fraction and simplified testing of high-flow-rate thrusters in ground facilities [31]. Bismuth is also roughly 1000th the cost of xenon and is significantly more readily available.

With this in mind, the shear-based transport model, with fitting parameters consistent with the Stanford Hall thruster at 200 V ( $C = 16 \times 10^{-8}$  s,  $\omega\tau_{\text{fluc}} = 8$ , and  $\alpha = 2$ ), has been used to simulate a Hall thruster designed to operate using bismuth propellant instead of xenon. In addition to the differing propellant, the simulation uses a slightly different geometry with a channel length of 2.4 cm instead of the 8-cm channel analyzed in the previous sections; early simulations indicated that a shorter channel would improve the efficiency of the bismuth thruster, and the channel length chosen mimics the design of a laboratory-model thruster modified for bismuth propellant [34]. Applying the shear-based transport model to this design provides a means of qualitatively understanding the effect of the different mass and ionization rate of the propellant gas.

Table II illustrates the performance characteristics of the xenon and bismuth hybrid simulations, both operating with the reduced channel length and at a discharge potential of 200 V. Note that these simulations were conducted neglecting the effects of charge-exchange collisions and background gas. Also, the bismuth simulation uses a larger mass flow rate to simulate the same number flow rate introduced at the anode of the xenon simulation.

In addition to providing more thrust per ion accelerated over the same potential drop, the bismuth thruster has the added advantage of a lower ionization potential resulting in higher

TABLE II  
COMPARISON OF SIMULATED PERFORMANCE PARAMETERS FROM XENON AND BISMUTH 2-D HYBRID HALL THRUSTER SIMULATIONS

	Bismuth	Xenon
Thrust [mN]	35.3	17.3
Current [A]	3.38	3.41
$I_{\text{sp}}$ [s]	1134	882
Total Efficiency	0.409	0.267

plasma density and propellant efficiency. The neutral density on the centerline at the exit plane of the 2.4-cm channel is an order of magnitude lower with bismuth propellant than xenon propellant. At all locations inside the channel, the plasma density is found to be higher for the bismuth thruster than for the xenon thruster. Although one might expect the bismuth-specific impulse to be roughly 21% lower than that for xenon due to the lower exhaust velocity associated with heavier particles, the propellant utilization of the simulated bismuth thruster is sufficiently high in that the  $I_{\text{sp}}$ , computed by dividing total thrust by mass flow rate and gravity, is found to be 28% higher for bismuth. A xenon thruster does benefit from a channel longer than 2.4 cm, and a simulated 8-cm channel running xenon provides an  $I_{\text{sp}}$  of 1227 s; the performance advantage here is only 8% over that of bismuth, again indicating the effect of bismuth's higher propellant utilization. Likewise, the thrust calculated for the bismuth thruster is roughly double that of the xenon thruster (rather than only 26% higher) owing to the increased number of accelerated ions. The calculated efficiency for the bismuth thruster indicates a 50% benefit compared to the xenon thruster.

#### IV. SUMMARY

Motivated by the observations and analytical work of the magnetic confinement fusion community, an empirical model for electron cross-field transport has been implemented in 2-D hybrid Hall thruster simulations based on the axial shear rate of the electron fluid. It is believed that the shearing of the fluid, caused by electric and magnetic field gradients, reduces the fluctuation-enhanced anomalous transport through stretching and distortion of turbulent eddies.

It has been shown that implementation of a shear-based transport barrier, which is computed locally and updated continuously, produces reasonable agreement with laboratory measurements. Despite a broader simulated transport barrier than experimentally observed, simulations using the shear-based approach produce similar profiles of properties such as electron temperature and potential as simulations using the experimental mobility. In all cases, the empirical shear-based transport model more accurately predicts plasma properties than a simple Bohm Hall parameter lacking any barrier to cross-field transport.

In order to evaluate the utility of this method, which relies on the unknown fitting parameters  $\omega\tau_{\text{fluc}}$  and  $C$ , an assessment was made of the sensitivity of the results to changes in these coefficients, as well as to the exponential dependence of the shear term and to assumptions made in the implementation of the model. For the specific conditions examined, it was found that plasma properties were fairly insensitive to the base value of anomalous transport  $\omega\tau_{\text{fluc}}$  and more largely dependent on the constant  $C$ , which is likely related to the growth rate of the instability which produces transport.

To assess the validity and portability of the model, the shear-based inverse Hall parameter has been implemented in simulations of an SPT-100 Hall thruster and was found to overpredict the thrust by as much as 30% and underpredict the efficiency by as much as 25%. The shear-based model has also been incorporated into a simulation of a bismuth Hall thruster in order to assess the effect of the heavier propellant and lower ionization cost. Results are in qualitative agreement with expectations, although data on bismuth are not available for a full quantitative comparison. Clearly, additional work is needed to identify a model that is transportable with accurate predictive capability. We believe that the shear model, if implemented with little time averaging, has the potential to do so, but at this time, time averaging is needed to stabilize the numerical simulation.

## REFERENCES

- [1] N. B. Meezan, W. A. Hargus, and M. A. Cappelli, "Anomalous electron mobility in a coaxial Hall discharge plasma," *Phys. Rev. E, Stat. Phys. Plasmas Fluids Relat. Interdiscip. Top.*, vol. 63, no. 2, p. 026410, Feb. 2001.
- [2] N. Gascon, M. Dudeck, and S. Barral, "Wall material effects in stationary plasma thrusters. I. Parametric studies of an SPT-100," *Phys. Plasmas*, vol. 10, no. 10, pp. 4123–4136, Oct. 2003.
- [3] S. Barral, K. Makowski, Z. Peradzynski, N. Gascon, and M. Dudeck, "Wall material effects in stationary plasma thrusters. II. Near-wall and in-wall conductivity," *Phys. Plasmas*, vol. 10, no. 10, pp. 4137–4152, Oct. 2003.
- [4] G. Janes and R. Lowder, "Anomalous electron diffusion and ion acceleration in a low-density plasma," *Phys. Fluids*, vol. 9, no. 6, pp. 1115–1123, Jun. 1966.
- [5] A. Wootton, B. Carreras, H. Matsumoto, K. McGuire, W. Peebles, C. Ritz, P. Terry, and S. Zweben, "Fluctuations and anomalous transport in tokamaks," *Phys. Fluids, B Plasma Phys.*, vol. 2, no. 12, pp. 2879–2903, Dec. 1990.
- [6] M. Cappelli, N. Meezan, and N. Gascon, "Transport physics in Hall plasma thrusters," presented at the 40th Aerospace Sciences Meeting, Reno, NV, 2002, AIAA-2002-0485.
- [7] P. Terry, "Suppression of turbulence and transport by sheared flow," *Rev. Modern Phys.*, vol. 72, no. 1, pp. 109–165, Jan. 2000.
- [8] E. Sommier, M. Scharfe, N. Gascon, M. Cappelli, and E. Fernandez, "Simulating plasma-induced Hall thruster wall erosion with a two-dimensional hybrid model," *IEEE Trans. Plasma Sci.*, vol. 35, no. 5, pp. 1379–1387, Oct. 2007.
- [9] S. Jachmich, M. V. Schoor, and R. Weynants, "On the causality between transport reduction and induced electric fields in the edge of a tokamak," presented at the 39th Conf. Plasma Phys. Control. Fusion, Montreux, Switzerland.
- [10] T. Hahn, "Physics behind transport barrier theory and simulations," *Plasma Phys. Control. Fusion*, vol. 44, no. 5A, pp. A87–A101, May 2002.
- [11] C. Thomas, "Anomalous electron transport in the Hall-effect thruster," Ph.D. dissertation, Stanford Univ., Stanford, CA, Oct. 2006.
- [12] E. Fernandez, M. Cappelli, and K. Mahesh, "2D simulations of Hall thrusters," in *Proc. CTR Annu. Res. Briefs*, 1998, p. 81.
- [13] M. Scharfe, N. Gascon, M. Cappelli, and E. Fernandez, "Comparison of hybrid Hall thruster model to experimental measurements," *Phys. Plasmas*, vol. 13, no. 8, pp. 083 505-1–083 505-12, Aug. 2006.
- [14] J. Fife, "Nonlinear hybrid-PIC modeling and electrostatic probe survey of Hall thrusters," Ph.D. dissertation, MIT, Cambridge, MA, 1998.
- [15] D. Bohm, E. Burhop, and H. Massey, *The Characteristics of Electrical Discharges in Magnetic Fields*. New York: McGraw-Hill, 1949, p. 13.
- [16] J. Boeuf and L. Garrigues, "Low frequency oscillations in a stationary plasma thruster," *J. Appl. Phys.*, vol. 84, no. 7, p. 3541, Oct. 1998.
- [17] C. Ritz, H. Lin, T. Rhodes, and A. Wootton, "Evidence for confinement improvement by velocity-shear suppression of edge turbulence," *Phys. Rev. Lett.*, vol. 65, no. 20, pp. 2543–2546, 1990.
- [18] E. Synakowski, S. Batha, M. Beer, M. Bell, R. Bell, R. Budny, C. Bush, P. Efthimion, T. Hahn, and G. Hammett, "Local transport barrier formation and relaxation in reverse-shear plasmas on the tokamak fusion test reactor," *Phys. Plasmas*, vol. 4, no. 5, pp. 1736–1744, May 1997.
- [19] H. Biglari, P. Diamond, and P. Terry, "Influence of sheared poloidal rotation on edge turbulence," *Phys. Fluids, B Plasma Phys.*, vol. 2, no. 1, pp. 1–4, Jan. 1990.
- [20] Y. Zhang and S. Mahajan, "Edge turbulence scaling with shear flow," *Phys. Fluids, B Plasma Phys.*, vol. 4, no. 6, pp. 1385–1387, Jun. 1992.
- [21] A. S. Ware, P. W. Terry, P. H. Diamond, and B. A. Carreras, "Transport reduction via shear flow modification of the cross phase," *Plasma Phys. Control. Fusion*, vol. 38, no. 8, pp. 1343–1347, Aug. 1996.
- [22] P. Terry, D. Newman, and A. Ware, "Suppression of transport cross phase by strongly sheared flow," *Phys. Rev. Lett.*, vol. 87, no. 18, p. 185 001, Oct. 2001.
- [23] K. Burrell, "Effects of  $E \times B$  velocity shear and magnetic shear on turbulence and transport in magnetic confinement devices," *Phys. Plasmas*, vol. 4, no. 5, pp. 1499–1518, 1996.
- [24] P. Terry, "Does flow shear suppress turbulence in nonionized flows?" *Phys. Plasmas*, vol. 7, no. 5, pp. 1653–1661, May 2000.
- [25] M. Scharfe, C. Thomas, D. Scharfe, N. Gascon, M. Cappelli, and E. Fernandez, presented at the 43rd Joint Propulsion Conf. & Exhibit, Washington, DC, 2007, AIAA-2007-5208.
- [26] A. Ware, P. Terry, B. Carreras, and P. Diamond, "Turbulent heat and particle flux response to electric field shear," *Phys. Plasmas*, vol. 5, no. 1, pp. 173–177, Jan. 1998.
- [27] R. Waltz, G. Staebler, W. Dorland, G. Hammett, M. Kotschenreuther, and J. A. Konings, "A gyro-Landau-fluid transport model," *Phys. Plasmas*, vol. 4, no. 7, pp. 2482–2496, Jul. 1997.
- [28] J. Fox, A. Batishcheva, O. V. Batishchev, and M. Martinez-Sanchez, "Adaptively meshed fully-kinetic PIC–Vlasov model for near vacuum Hall thrusters," presented at the 42nd Aerospace Sciences Meeting and Exhibit, Washington, DC, 2006, AIAA-2006-4324.
- [29] A. Smith and M. Cappelli, "Advancing propulsion technologies and celebrating our aerospace heritage," presented at the 43rd Joint Propulsion Conf. & Exhibit, Washington, DC, 2007, AIAA-2007-5240.
- [30] J. Sankovic, J. Hamley, and T. Haag, "Performance evaluation of the Russian SPT-100 at NASA LeRC," presented at the 23rd Int. Electric Propulsion Conf., Seattle, WA, 1993, IEPC-93-094.
- [31] S. Tverdokhlebov, A. Semenkin, and J. Polk, "Bismuth propellant option for very high power TAL thruster," presented at the 40th Aerospace Sciences Meeting, Washington, DC, 2002, AIAA-2002-0348.
- [32] S. D. Grishin, V. S. Erofeev, A. V. Zharinov, V. P. Naumkin, and I. N. Safronov, "Characteristics of a two-stage ion accelerator with an anode layer," *J. Appl. Mech. Tech. Phys.*, vol. 19, no. 2, pp. 166–173, Mar. 1978.
- [33] J. Dunning, "NASA's electric propulsion program—Technology investments for the new millennium," presented at the 37th Joint Propulsion Conf., Salt Lake City, UT, 2001, AIAA-2001-3224.
- [34] D. B. Scharfe and M. A. Cappelli, "Stationary reference Bi discharge cell for optical diagnostics of a bismuth fueled Hall thruster," presented at the 29th Int. Electric Propulsion Conf., Princeton, NJ, 2003, IEPC-2005-058.



**Michelle K. Scharfe** received the B.S. degree in engineering and applied science from the California Institute of Technology, Pasadena, in 2003 and the M.S. degree in mechanical engineering from Stanford University, Stanford, CA, in 2005, where she is currently working toward the Ph.D. degree in the Mechanical Engineering Department.

Her research interests focus on improving Hall thruster simulations through inclusion of more accurate physics, particularly in the areas of electron transport, heavy-particle dynamics, and electron–

wall interactions.



**Cliff A. Thomas** received the B.S. degree in mechanical engineering from Rice University, Houston, TX, and the M.S. and Ph.D. degrees in mechanical engineering from Stanford University, Stanford, CA.

He is currently a Research Scientist with the Lawrence Livermore National Laboratory, Livermore, CA, studying target physics for the National Ignition Facility. His research interests include transport physics in magnetized and unmagnetized plasmas, wave dynamics, and numerical methods.



**David B. Scharfe** received the B.S. degree in mechanical engineering from the University of Southern California, Los Angeles, in 2003 and the M.S. degree in mechanical engineering from Stanford University, Stanford, CA, in 2005, where he is currently working toward the Ph.D. degree in the Mechanical Engineering Department.

His research includes simulations of and experiments with bismuth metal vapor plasma devices, and his experimental work includes optical and probe-based diagnostics of various plasmas.



**Nicolas Gascon** received the Ph.D. degree in radiation and plasma physics from the University of Provence, Marseilles, France.

He has been with the Stanford Plasma Physics Laboratory, Mechanical Engineering Department, Stanford University, Stanford, CA, from 2001 to 2008 and is currently with Space Systems/Loral, Palo Alto, CA. His research projects focus on understanding the physics of magnetized discharges, anomalous electron transport, plasma-wall interactions, and developing novel plasma propulsion

concepts.



**Mark A. Cappelli** received the B.A.Sc. degree in physics from McGill University, Montreal, QC, Canada, and the M.A.Sc. and Ph.D. degrees in aerospace science from the University of Toronto, Toronto, ON, Canada.

He has been with Stanford University, Stanford, CA, since 1987, where he is currently a Professor of mechanical engineering in the Mechanical Engineering Department. His research interests include plasma physics and spectroscopy, plasma propulsion, plasma-assisted combustion, and plasma-assisted

material synthesis.



**Eduardo Fernandez** received the B.S. degree in physics and mathematics from the University of Wisconsin, Eau Claire, and the Ph.D. degree in physics from the University of Wisconsin, Madison.

He did postdoctoral work on plasma simulation at the Center for Turbulence Research, Stanford University, Stanford, CA. His interests include turbulence in fluids and plasmas, plasma modeling, and simulation. He is currently an Associate Professor of physics and mathematics with Eckerd College, St. Petersburg, FL, where he has been working

since 1999.